Fourth International Conference on FRP Composites in Civil Engineering (CICE2008)
22-24July 2008, Zurich, Switzerland

CFRP group effect and interaction between stirrups and strips on the NSM-shear strengthening of RC beams

A.C.T. Gomes, J.A.O. Barros
ISISE, Depart. Civil Eng., University of Minho, Guimarães, Portugal

J.P.S.E. Dias
Civitest Company, Celeiros, Braga, Portugal

ABSTRACT: Available experimental research shows that the technique based on installing Carbon Fibre Reinforced Polymer (CFRP) strips into slits opened on the cover concrete of the beam's lateral faces, designated as Near Surface Mounted (NSM), is very effective to increase the shear resistance of reinforced concrete (RC) beams. However, recent research has revealed that, in terms of NSM shear strengthening effectiveness, a detrimental effect can occur between existing steel stirrups and applied strips, as well as amongst the strips when the distance between strips, s_f, is lower than a certain limit. In the present work, a test setup was developed and an experimental program was carried out to assess the influence of both s_f and interaction between existing steel stirrups and strips on the shear strengthening of RC beams. The experimental program is described and the main results are presented and analyzed.

1 INTRODUCTION

To assess the influence of both the distance between consecutive CFRP strips, s_f, and the percentage of existing steel stirrups, ρ_{sw}, on the NSM shear strengthening effectiveness, using a relatively simple test setup, the hypothesised approach schematically illustrated in Figure 1 was adopted in the present work. The specimen has a diameter of 600 mm and a thickness of 180 mm, equal to the thickness of the web of the RC beams tested in previous experimental programs (Dias & Barros 2006, Dias et al. 2007). This specimen is subjected to a loading plane, able to form a crack plane that forms an angle with the direction of existing steel stirrups similar to the one observed in the tested RC beams. The effectiveness of the NSM shear strengthening technique can be evaluated from the: maximum load supported by the specimens; strain profile and maximum strain in the strips during the specimen loading process. Furthermore, the influence of the relative orientation between strips and diagonal crack on the NSM effectiveness can be easily assessed adopting this test setup.

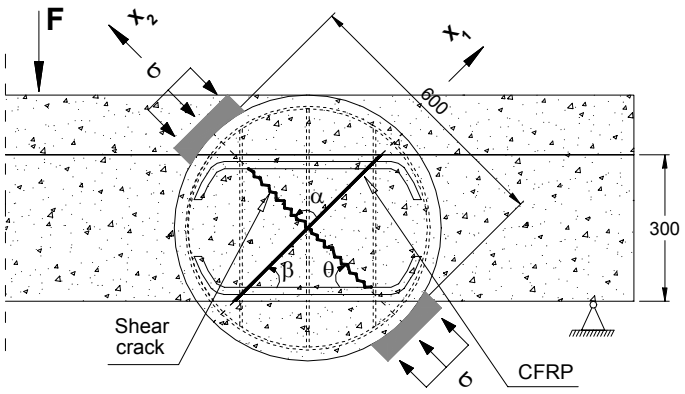

Figure 1. Idealization of a test setup for the capture of the phenomena in discussion (dimensions in mm).

2 EXPERIMENTAL PROGRAM

2.1 *Series*

Figure 2 represents the specimen characteristics of the test series of the experimental program. LXSY is the generic designation of a tested specimen, where X and Y are the number of CFRP strips and stirrups, respectively. For instance, L4S3 is the specimen with 4 strips and 3 stirrups.

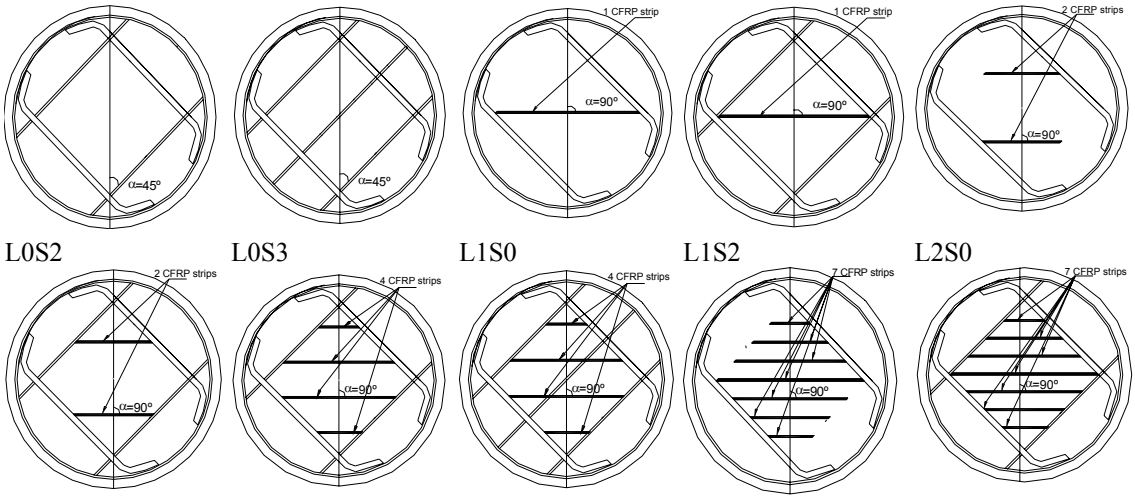

L0S2 L0S3 L1S0 L1S2 L2S0

L2S2 L4S2 L4S3 L7S0 L7S2

Figure 2. Specimens of the experimental program.

Figure 3 represents details of the steel reinforcement that w asarranged in order to reproduce, as much as possible, the reinforcement arrangement in a shear critical zone of a T cross section beam (see also Figure 1). The steel stirrups were extended to the top part of the specimen in order to simulate the anchorage conditions found in a T beam, where the stirrups embrace the top longitudinal reinforcement placed in the beam's flange. To avoid undesirable premature failures, stirrups were also placed in the bottom part of the specimen, outside the testing zone, and two steel bars of 6 mm diameter were positioned along the contour of the specimen. The preparation of the specimens and the strengthening procedures are described elsewhere (Barros & Oliveira 2007).

2.2 *Test Setup, Monitoring Strategy and Test Procedures*

As Figure 4b shows, the direction of the failure crack was assumed as making an angle of 45 degrees with the steel stirrups, which is in agreement with the assumption adopted in some analytical models dedicated to the evaluation of the contribution of FRP systems for the shear resistance of RC beams (ACI 2002; CNR-DT 200 2004; fib 2001). To form this failure crack, using a servo-controlled machine of load carrying capacity of 2000 kN in compression (Figure 4a), the specimens were installed in the equipment in such a way that the vertical loading axis coincided with the direction of the failure crack to be formed (Figures 1 and 4b). To avoid excessive stress concentration in the specimen zones subjected to the influence of the machine loading platens, two intermediate steel supports, with a surface configuration adjusted to the geometry of the specimen (thickness equal to the specimen and a width of 170 mm), were interposed between these platens and the specimen (Figure 4b).

Figure 5 indicates the positions of the strain gauges installed on the steel stirrups and on the CFRP strips. On each face of the specimen, two LVDTs were placed, one to measure the vertical deformation and the other the horizontal deformation (see Figure 4b). The measuring length of both the vertical and horizontal LVDTs was 424 mm. Another vertical LVDT was used to control the test at a displacement rate of 2μm/s. The applied force was measured by a load cell of 2000 kN capacity.

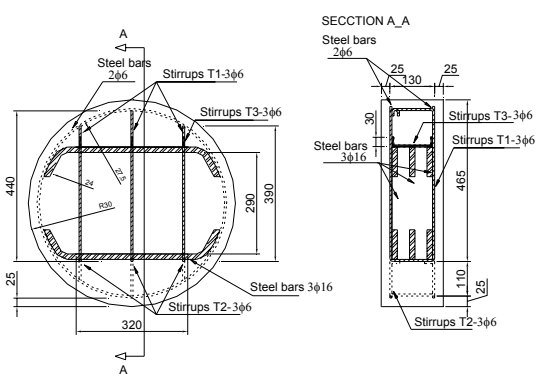

Figure 3. Arrangement of the conventional reinforcement (dimensions in mm).

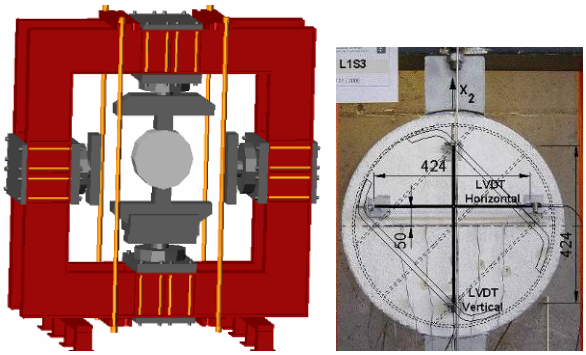

a) b)

Figure 4. (a) Equipment and (b) test setup (dimensions in mm).

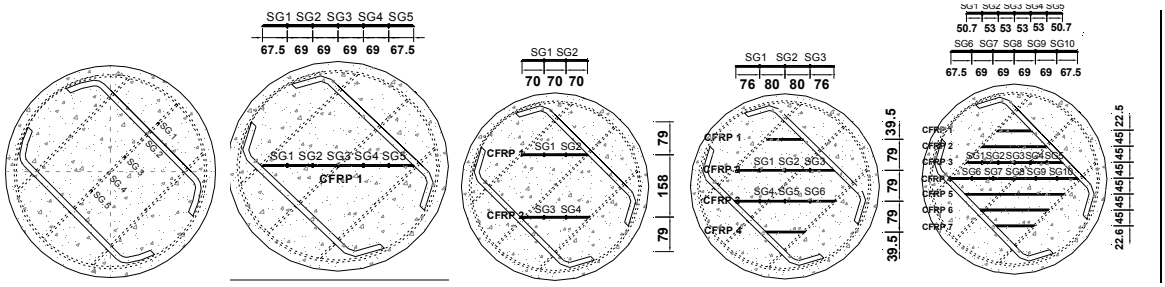

a) b) c) d) e)

Figure 5. Strain gauges applied on the: a), steel stirrups; b) c), d), e) CFRP strips (dimensions in mm).

2.3 *Material Properties*

In this experimental program a concrete strength class C20/25 was used, supplied by a Ready-Concrete Central (f_{ck}=20 MPa and E_c=29 GPa at 28 days). To evaluate the tensile properties of the steel bars reinforcing the specimens, tensile tests were carried out according to the EN 10 002-1 recommendations (1990). For the elasticity modulus, yield stress and tensile strength of 6 and 16 mm diameter steel coupons, the following values were obtained: 198.04 (2.11) GPa [1.07%], 439.58 (7.30) MPa [1.66%], 568.28 (7.01) MPa [1.22%] – for ∅6 mm; 196.61 (17.81) GPa [9.06%], 405.90 (2.98) MPa [0.73%], 553.84 (7.01) MPa [1.03%] – for ∅16 mm, where the values between round and square brackets are the standard deviation (SD) and the coefficient of variation [COV], respectively.

The CFRP strips were supplied by the S&P Company, and had a cross section of 10×1.4 mm^2. Four tests were carried out according to the ISO 527-5 recommendations (1997), from which the following average values were obtained: tensile strength (f_{fu}) of 2879 MPa; elasticity modulus (E_f) of 156.1 GPa; and strain at peak stress (ε_{fu}) of 18.4‰.

From nine tensile tests with specimens of the epoxy adhesive used to bond the strips to the concrete substrate, carried out according to ISO 527-2 recommendations (1993), an average tensile strength of 33.03 MPa (with a SD of 2.81 MPa and a COV of 5.76%); an average modulus of elasticity of 7.47 GPa (with a SD of 0.32 GPa and a COV of 4.28%); and an average ultimate strain of 4.83‰ (with a SD of 0.57‰ and a COV of 11.8%) were obtained (Bonaldo et al. 2006).

2.4 *Results and discussion*

Figure 6 includes the relationships between the applied force and the strains measured through the use the LVDTs in both vertical and horizontal directions (negative values correspond to compressive strains). Each curve is the average of the displacement values recorded in the corresponding LVDTs placed on the front and rear faces of the specimen, divided by the LVDT measuring length (424 mm). The main obtained results are included in Table 1, where F_{cr} is considered the load at the moment when crack formation was visible (in general corresponds to

a drop on the force-deflection curve), F_{max} is the maximum load, $\varepsilon_{c,hor}^{F_{max}}$ is the horizontal strain at F_{max}, $\varepsilon_{c,hor}^{Max}$ is the maximum measurable horizontal strain, $\varepsilon_{c,ver}^{F_{max}}$ is the vertical strain at F_{max}, $\varepsilon_{c,ver}^{Max}$ is the maximum measurable vertical strain, $\varepsilon_{f}^{F_{max}}$ is the average strain in the strips at F_{max}, $\varepsilon_{f,\max}^{F_{max}}$ is the maximum strain in the strips at F_{max}, ε_{f}^{Max} is the maximum strain value in the strips and $\tau_{bm,\max}^{RL,F_{max}}$ is the maximum value of the bond stress at F_{max}. The bond stress τ_{bm}^{RL} in a strip, in-between the strain gauges positioned at SGL (left) and SGR (right), was determined according to the following equation (see scheme inset of Figure 9a):

$$\tau_{bm}^{RL} = \frac{E_f \cdot A_f \cdot \Delta\varepsilon^{RL}}{2 \cdot w_f \cdot L^{RL}} \tag{1}$$

where L^{RL} is the distance between two consecutive strain gauges; $\Delta\varepsilon^{RL}$ is the axial strain difference between the strain gauge at right (ε^R) and left (ε^L) sections; and w_f is the width of the strip, respectively. In this approach, constant bond stress between SGL and SGR is assumed.

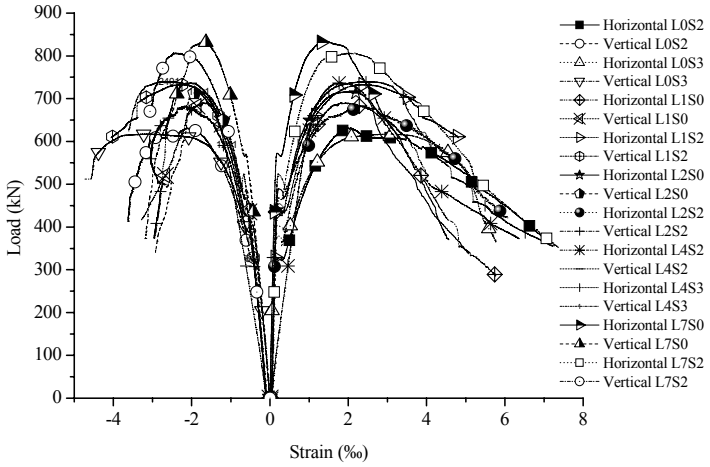

Figure 6. Force versus vertical and horizontal strains.

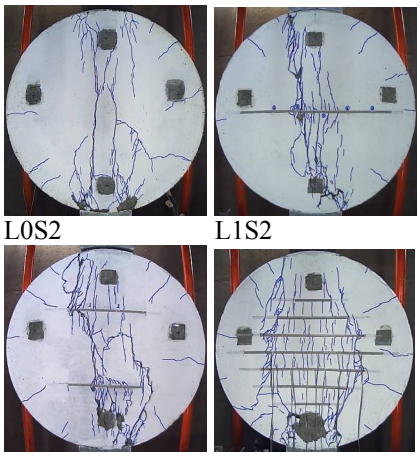

Figure 7. Typical failure modes.

From the analysis of Figure 6 it is observed that all the tested specimens had similar deformational behaviour. In fact, up to the formation of the macro-crack that occurred near the loading plane, at a load level that ranged from 325 kN to 571 kN, the deformational behaviour was almost linear. A tendency for an increase of F_{max} with the increase of the CFRP percentage (ρ_{fw}) is apparent from the values in Table 1 and from Figure 8a.

Due to circumferential tensile stresses developed at the contour of the specimen, some radial cracks have formed (see Figure 7). At the formation of the main crack, apart from the L4S2 specimen, an abrupt decay of stiffness occurred, followed by a "hardening branch" of a stiffness that depended, mainly, on the ρ_{fw}. The maximum load, F_{max}, that ranged from [617-833] kN occurred at specimen vertical and horizontal strains that ranged from [1.7-3.4]‰ and [1.9-3.2]‰, respectively. After peak load, the specimen entered in a softening phase up to an axial vertical deformation that varied from 2.9 to 5.5 ‰. Figure 8a shows that the effectiveness of the NSM in terms of F_{max} decreased with the increase of the percentage of steel stirrups, confirming the detrimental effect of the interaction strips-stirrups, already observed in other experimental programs (Bianco et al. 2006). Figure 8b shows that, in general, the horizontal deformability of the specimens at peak load, ($\varepsilon_{c,hor}^{F_{max}}$) increases with the number of strips bridging the critical failure crack, but only up to a certain ρ_{fw}, since after this ρ_{fw} the stiffness increment provided by the strips has decreased the ductility of the specimens. If NSM strengthening effectiveness can be measurable from the average strains installed in the strips at F_{max}, Figure 8c shows that, for strips almost orthogonal to the critical crack, above a ρ_{fw} around 0.06 the strains that can be applied to the strips decrease, which means that the NSM effectiveness decreases above this ρ_{fw}. This effectiveness decrement can be also observed from the relationship between ρ_{fw} and the maximum bond stress at F_{max} ($\tau_{bm,\max}^{RL,F_{max}}$), represented in Figure 8d.

Table 2. Main obtained results

Ref.	ρ_{fw} [1]	F_{cr} (kN)	F_{max} (kN)	$\varepsilon_{c,hor}^{F_{max}}$ (‰)	$\varepsilon_{c,hor}^{Max}$ (‰)	$\varepsilon_{c,ver}^{F_{max}}$ (‰)	$\varepsilon_{c,ver}^{Max}$ (‰)	$\varepsilon_{f}^{F_{max}}$ (‰)	$\varepsilon_{f,\max}^{F_{max}}$ (‰)	ε_{f}^{Max} (‰)	$\tau_{bm,\max}^{RL,F_{max}}$ (MPa)
L0S2		325	630	2.033	6.934	2.063	3.625				
L0S3		415	617	3.160	5.772	3.439	4.579				
L1S0	0.0259	520	690	1.851	4.551	1.703	3.291	2.333	6.756	9.919	3.538
L1S2	0.0259	455	733	2.393	7.303	2.259	5.493	2.891	6.175	9.129	4.095
L2S0	0.0519	488	716	2.085	5.074	1.870	2.938	5.399	6.271	10.178	3.625
L2S2	0.0519	375	685	2.392	6.080	2.184	3.047	4.225	6.940	7.975	3.485
L4S2	0.1037	-	736	1.870	6.351	2.088	2.962	3.276	5.148	7.359	2.961
L4S3	0.1037	445	739	2.712	3.841	2.780	3.631	4.618	7.046	8.610	3.537
L7S0	0.1815	571	833	1.438	3.244	1.715	6.384	2.048	5.111	7.657	2.618
L7S2	0.1815	467	807	2.177	7.374	2.466	3.084	2.732	4.594	5.592	3.244

(1) $\rho_{fw} = A_f \Big/ \left(b_w \times s_f \times \sin\alpha\right) = \left(2\times 10\times 1.4\right) \Big/ \left(180\times s_f \times \sqrt{2}/2\right)\times 100$

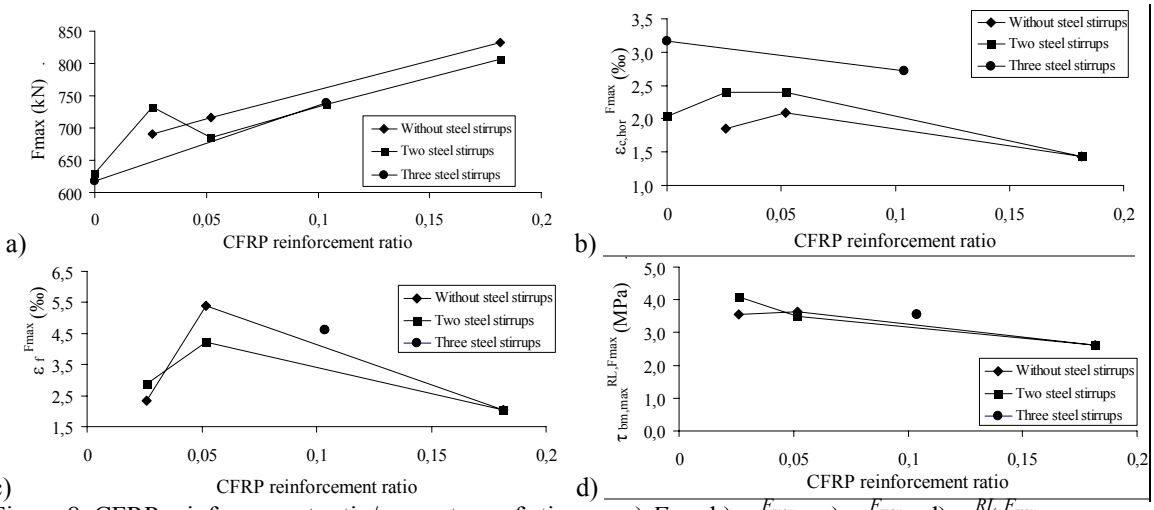

Figure 8. CFRP reinforcement ratio/percentage of stirrups: a) F_{max}; b) $\varepsilon_{c,hor}^{F_{max}}$; c) $\varepsilon_{f}^{F_{max}}$; d) $\tau_{bm,\max}^{RL,F_{max}}$.

The τ_{bm}^{RL} variation during the loading process of the L1S2 specimen is shown in Figure 9b, from which it is observed that at crack initiation an abrupt increase of the maximum bond stress occurred. As expected, the bond stress decreases from the centre of the CFRP strip (that coincides with the loading plane) up to the extremity of the strip, due to the formation and propagation of a crack band width along the loading plane. The decrease rate of τ_{bm}^{RL} from the centre to the extremity increases with the increase of the applied load. Table 1 shows that the maximum τ_{bm}^{RL} at F_{max} is around 4.5 MPa.

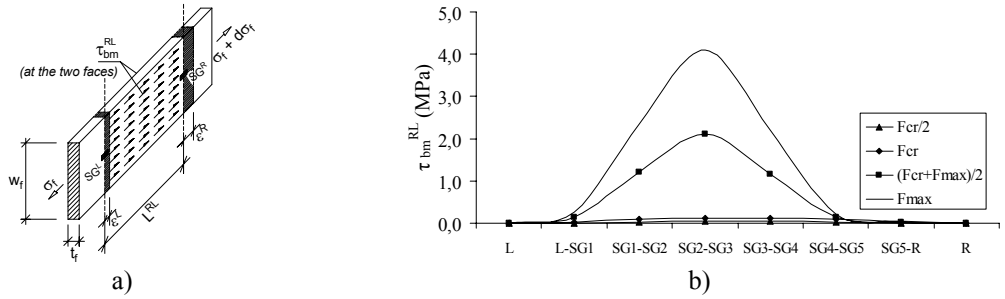

Figure 9. Bond stress: a) how it was determined; b) variation at distinct force levels for the L1S2.

Figure 7 represents typical crack patterns observed in the carried out tests. The formation of a diffuse crack pattern is visible in the concrete surrounding the strips due to the stress transfer between these materials. This tendency has accentuated with the increase of the CFRP percentage. For the highest CFRP percentage, the concrete layer reinforced with the strips has almost sepa-

rated from the concrete core of the specimen, due to a group effect already observed in RC beams shear strengthened according to the NSM technique (Dias and Barros 2006). This indicates that concrete strength and s_f limit the contribution of the NSM strips for the shear strengthening, confirming analytical research in development (Bianco et al. 2007).

3 CONCLUSIONS

A new test setup was proposed to estimate the influence of the spacing between NSM CFRP strips, s_f, and the detrimental effect between strips and existing steel stirrups, in terms of the effectiveness of the NSM shear strengthening technique for RC beams. The obtained results confirmed the existence of a minimum s_f, below which a group effect is a mandatory mechanism that leads to a failure mode by the detachment of the concrete cover that includes the strips. The obtained results have also revealed that the presence of existing steel stirrups decreases the effectiveness of the NSM shear strengthening technique, and the loss of effectiveness increased with the increase of the percentage of existing steel stirrups. A larger experimental program needs to be carried out in order to quantify the optimal s_f, as well as the detrimental effect of the presence of the steel stirrups.

4 ACKNOWLEDGMENTS

The authors wish to acknowledge the support provided by the "Empreiteiros Casais", S&P®, Secil (Unibetão, Braga). The study reported in this paper forms a part of the research program "SmartReinforcement – Carbon fibre laminates for the strengthening and monitoring of reinforced concrete structures" supported by ADI-IDEIA, Project nº 13-05-04-FDR-00031.

5 REFERENCES

American Concrete Institute. 2002. *Guide for the Design and Construction of Externally Bonded FRP Systems for Strengthening Concrete Structures*. ACI 440.2R-02, Farmington Hills, MI.

Bianco, V., Barros, J.A.O., Monti, G. 2006. Shear Strengthening of RC beams by means of NSM laminates: experimental evidence and predictive models. *Technical report 06-DEC/E-18*, Dep. Civil Eng., School Eng. University of Minho, Guimarães- Portugal.

Bianco, V., Barros, J.A.O. and Monti, G. 2007. A new approach for modeling the NSM shear strengthening contribution in reinforced concrete beams. *FRPRCS-8*, Univ. Patras, Greece,16-18 July, ID 8-12.

Barros, J.A.O., and Oliveira, J.T. 2007. A test setup to assess the influence of mandatory parameters affecting the performance of NSM CFRP laminates for the shear strengthening of RC beams. *Proceedings of ACIC 07*, Advanced Composites in Construction, Univ. of Bath, Bath, UK, 282-291 2–4 April.

Bonaldo, E., Barros, J.A.O., and Lourenço, P.B. 2006. Strengthening technique combining CFRP laminates and compressive overlayer of steel fibre reinforced concrete to increase the flexural resistance of RC slabs. *Technical report 06-DEC/E-05,* Dep. Civil Eng., School Eng. University of Minho, 104 p.

CNR-DT 200. 2004. *Guidelines for design, execution and control of strengthening interventions by means of fibre reinforced composites*. National Research Council - advisory Committee on technical regulations for constructions, CNR.

Dias, S.J.E., and Barros, J.A.O. 2006. NSM CFRP Laminates for the Shear Strengthening of T Section RC Beams. *2nd International fib Congress*, Naples, Italy, ID 10-58.

Dias, S.J.E., Bianco, V., Barros, J.A.O., and Monti, G. 2007. Low strength concrete T cross section RC beams strengthened in shear by NSM technique. *Workshop*, Univ. of Salerno, Italy, 12-13 February.

EN 10 002–1. 1990. *CEN: Metallic materials – Tensile testing. Part 1: Method of test (at ambient temperature)*, Brussels, 35 p.

fib Bulletin 14. 2001. *Externally Bonded FRP reinforcement for RC structures*. Technical report, Task Group 9.3 FRP reinforcement for concrete structures.

ISO 527-5. 1997. *Plastics - Determination of tensile properties - Part 5: Test conditions for unidirectional fibre-reinforced plastic composites*. International Organization for Standardization, Genève, Switzerland, pp 9.

ISO 527-2. 1993. *Plastics - Determination of tensile properties - Part 2: Test conditions for moulding and extrusion plastics*. International Organization for Standardization (ISO), Geneva, Switzerland.